Atmospheric Environment 63 (2012) 68–76

Contents lists available at SciVerse ScienceDirect

Atmospheric Environment

journal homepage: www.elsevier.com/locate/atmosenv

The secondary formation of inorganic aerosols in the droplet mode through heterogeneous aqueous reactions under haze conditions

Xinfeng Wang, Wenxing Wang*, Lingxiao Yang, Xiaomei Gao, Wei Nie, Yangchun Yu, Pengju Xu, Yang Zhou, Zhe Wang

Environment Research Institute, Shandong University, Ji'nan, Shandong 250100, China

HIGHLIGHTS

- Size-resolved inorganic aerosol compositions were analyzed for a highly polluted area.
- Humidity-dependent heterogeneous formation of inorganic aerosols was investigated.
- Relationships were given between the SO_4^{2-}, NO_3^-, NH_4^+ in the droplet mode and the RH.
- Dominant formation pathways of sulfates and nitrates were analyzed for haze events.

ARTICLE INFO

Article history:
Received 6 June 2012
Received in revised form
3 September 2012
Accepted 10 September 2012

Keywords:
Secondary inorganic aerosols
Mass size distribution
Droplet mode
Heterogeneous aqueous reaction
Haze pollution
Jinan

ABSTRACT

Secondary inorganic aerosols play important roles in visibility reduction and in regional haze pollution. To investigate the characteristics of size distributions of secondary sulfates and nitrates as well as their formation mechanisms under hazes, size-resolved aerosols were collected using a Micro-Orifice Uniform Deposit Impactor (MOUDI) at an urban site in Jinan, China, in all four seasons (December 2007–October 2008). In haze episodes, the secondary sulfates and nitrates primarily formed in fine particles, with elevated concentration peaks in the droplet mode (0.56–1.8 μm). The fine sulfates and nitrates were completely neutralized by ammonia and existed in the forms of $(NH_4)_2SO_4$ and NH_4NO_3, respectively. The secondary formation of sulfates, nitrates and ammonium (SNA) was found to be related to heterogeneous aqueous reactions and was largely dependent on the ambient humidity. With rising relative humidity, the droplet-mode SNA concentration, the ratio of droplet-mode SNA to the total SNA, the fraction of SNA in droplet-mode particles and the mass median aerodynamic diameter of SNA presented an exponential, logarithmic or linear increase. Two heavily polluted multi-day haze episodes in winter and summer were analyzed in detail. The secondary sulfates were linked to heterogeneous uptake of SO_2 followed by the subsequent catalytic oxidation by oxygen together with iron and manganese in winter. The fine nitrate formation was strongly associated with the thermodynamic equilibrium among NH_4NO_3, gaseous HNO_3 and NH_3, and showed different temperature-dependences in winter and summer.

1. Introduction

The size distribution of aerosols is crucial in understanding the particle emissions, *in-situ* formation and the subsequent conversion processes of secondary aerosols and is also important in assessing the effects of aerosols on human health and the global radiation budget (Salma et al., 2002; Mather et al., 2003; Liu et al., 2008; Haywood et al., 2008). Typically, the mass distribution is dominated by three modes (or sub-modes): the condensation mode (~0.1–0.5 μm), the droplet mode (~0.5–2 μm) and the coarse mode (~2–50 μm) (John et al., 1990; Seinfeld and Pandis, 2006; Guo et al., 2010).

Haze is defined as the weather phenomenon featuring a high concentration of fine particles that leads to horizontal visibility below 10 km at a relative humidity (RH) less than 90% (Wu, 2006). Haze pollution is characterized by the elevated levels and high fractions of the secondary components of sulfates, nitrates and ammonium (SNA) in fine particles (Sun et al., 2006; Wang et al., 2006; Tan et al., 2009). Generally, the sulfates are primarily produced through the gas-phase oxidation of SO_2 by the OH radical followed by nucleation and condensational growth, or are produced by the heterogeneous uptake of SO_2 on pre-existing particles or

* Corresponding author. Tel.: +86 531 88369788; fax: +86 531 88361990.
E-mail address: wenxwang@hotmail.com (W. Wang).

1352-2310/$ – see front matter © 2012 Elsevier Ltd. All rights reserved.
http://dx.doi.org/10.1016/j.atmosenv.2012.09.029

cloud droplets followed by being oxidized by O_3, H_2O_2, or O_2 catalyzed by Fe(III) and Mn(II) (Berresheim and Jaeschke, 1986; Mather et al., 2003; Seinfeld and Pandis, 2006; Yao and Zhang, 2011). The fine nitrate formation is dominated by the reactions of gaseous HNO_3 or nitric acid in droplets with NH_3 under ammonia-rich conditions or by heterogeneous hydrolysis of N_2O_5 on aerosol surfaces in ammonia-poor environments (Schryer, 1982; Seinfeld and Pandis, 2006; Pathak et al., 2009). Ammonium in fine mode particles is mostly combined with sulfates and/or nitrates (Feng and Penner, 2007). Several recent studies have emphasized the important roles of heterogeneous reactions in secondary aerosol formation during polluted scenarios. Field measurements during a wood smoke episode and the subsequent modeling simulation indicate the evidence of secondary sulfate formation via heterogeneous surface reactions on smoke particles (Buzcu et al., 2006). Both laboratory experiments and *in-situ* observations also indicate the importance of the aqueous oxidation of SO_2 catalyzed by metals in sulfate formation under humid conditions (Turšič et al., 2003; Li et al., 2011). During particulate matter (PM) pollution episodes, the dominant formation pathway of fine nitrates is found to vary with the location as well as with the sampling period and is strongly dependent on the ambient abundance of ammonia (e.g., Pathak et al., 2009; Wang et al., 2009; Ye et al., 2011). In polluted environments of high particle loading and high levels of gas precursors in China, the aerosol mass size distributions usually exhibit a sharp peak within the size range of 0.56–1.8 μm when fine particle pollution occurred (Hu et al., 2005; Huang et al., 2006; Guo et al., 2010; Cheng et al., 2011b). In spite of a large contribution of droplet-mode aerosols to the PM, field studies have rarely focused on the secondary formation of droplet-mode aerosols in such environments.

Jinan, the capital of the Shandong Province, has a population of 6.8 million and an area of 8177 square kilometers. It is located near the center of the North China Plain. The city is surrounded by mountains to the south and hills to the east (Fig. 1), which is disadvantageous for air pollutants to disperse. With the rapid urbanization and industrial development in the past several decades, Jinan has suffered from deteriorated air quality in particular, from heavy PM pollution (Yang et al., 2007; Cheng et al., 2011a). In 2008, the average aerosol optical depth over Jinan was very high – exceeding 0.6 (see Fig. 1a). The annual average $PM_{2.5}$ in urban Jinan was at a level of 124–156 μg m^{-3} (Cheng et al., 2011a). Sulfates, nitrates and ammonium, the dominant water-soluble ions, contributed approximately 47% of the fine particles. The elevated aerosol loading is responsible for reducing atmospheric visibility. Jinan experiences haze pollution on nearly one-third of the days in a year (Cheng et al., 2011b). Furthermore, the MODIS (moderate-resolution imaging spectroradiometer) true-color images of haze episodes over this area always show a regional-scale brown haze, covering most of the North China Plain (e.g., Li et al., 2011).

To obtain a comprehensive understanding of the droplet-mode aerosol formation and the involved chemical mechanisms, a large number of size-segregated aerosol samples were collected in an urban area in Jinan and underwent chemical analysis in the laboratory. We first compare the size-resolved aerosol compositions in haze episodes with those found on clear days to identify the characteristics of aerosol size distributions and chemical compositions for the haze pollution. Then, the humidity-dependent heterogeneous formation of SNA is analyzed, and the relationships between the droplet-mode SNA and the ambient humidity are given based on the field measurements. Two severe, multi-day haze episodes in winter and summer are also discussed in detail to investigate the dominant formation pathways of sulfates and nitrates in the droplet mode and to investigate the factors affecting the secondary aerosol formation.

2. Experiment and methods

2.1. Sampling site

Size-segregated aerosols were collected from an urban area of Jinan, China. The sampling site is located on the rooftop of a seven-story teaching building in the center campus of Shandong University (36.67° N, 117.05° E and 50 m asl) and is surrounded by a residential area. There are several large-scale industries in Jinan, including steel plants, thermal power plants, cement plants, oil refineries and chemical plants, which are considered the major industrial emission sources of the local air pollution. Size-resolved aerosol samples were collected discontinuously in all four seasons from November 2007 to October 2008. Normally, atmospheric aerosols were collected over 24-h periods every two or three days. When pollution episodes occurred, sample collection was increased to take place once or twice per day. During the sampling periods, the relative humidity in Jinan covered a large range of 8%–91%, and the temperatures varied from −2 to 32 °C.

2.2. Sample collection and analysis

In this study, a MOUDI (Micro-Orifice Uniform Deposit Impactor, Model 110 with rotator, MSP) was deployed to collect the aerosol samples at a flow rate of 30 L min^{-1}. The MOUDI has eight stages with size ranges of >18 μm (inlet), 10–18 μm, 5.6–10 μm, 3.2–5.6 μm, 1.8–3.2 μm, 1.0–1.8 μm, 0.56–1 μm, 0.32–0.56 μm, 0.18–

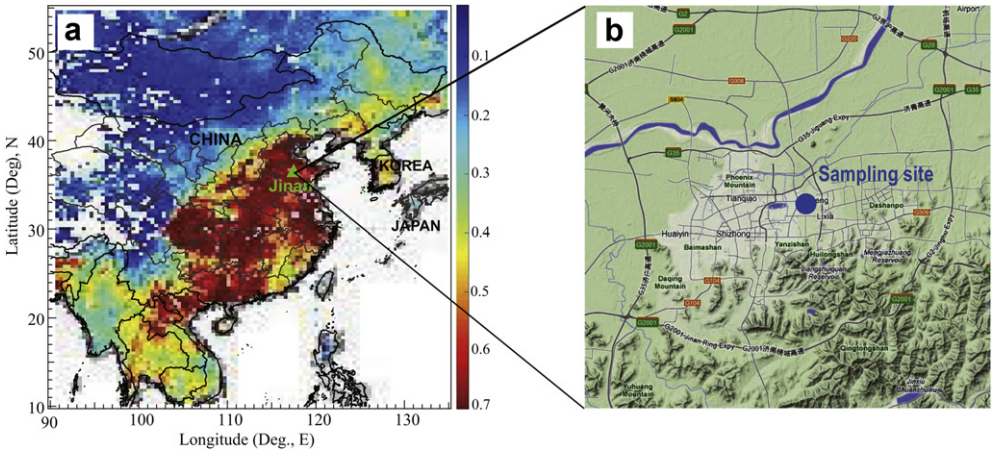

Fig. 1. Map showing the study area, (a) the aerosol optical depth in 2008 (http://aatsraerosol.fmi.fi/DwnLdPage_Globe.html) and (b) the location of our sampling site.

0.32 μm. Aluminum substrates (MSP) were used to collect the aerosol samples. Before sampling, the substrates were pre-heated to 500 °C using a muffle furnace to remove residual organics. After sampling, the aluminum substrates were placed in plastic Petri dishes and stored in a refrigerator at a temperature below −5 °C for subsequent gravimetric and chemical analysis in the laboratory. The substrates were then weighed using a microbalance (ME5, Sartorius). Before weighing, the substrates were balanced for 48 h with constant temperature (20 ± 0.5 °C) and relative humidity (50 ± 2%). As found in our previous study by Nie et al. (2010) during the summer in Beijing, the use of aluminum substrates in MOUDI sampler is subject to apparent evaporation loss for ammonium nitrates in high-temperature conditions. For the present study in Jinan, the temperature was moderate, and the sampling artifacts were generally less than 20%.

In the laboratory, the atmospheric aerosol samples collected on aluminum substrates were completely dissolved in deionized water by ultrasonication. Inorganic water-soluble ions in the sample solutions were detected using an ion chromatograph (ICS-90, Dionex). The anions, including F^-, Cl^-, NO_3^- and SO_4^{2-}, were analyzed using an AS14A Column with an AMMS 300 Suppresser and were eluted with 3.5 mmol L^{-1} Na_2CO_3–1.0 mmol L^{-1} $NaHCO_3$. The cations Na^+, NH_4^+, K^+, Mg^{2+} and Ca^{2+} were analyzed using a CS12A Column with a CSRS Ultra II Suppresser and were eluted with 20 mmol L^{-1} methanesulfonic acid.

Concurrently, a number of other air pollutants and parameters were measured during this study. SO_2 was measured using a pulsed UV fluorescence analyzer (Model 43C, TEC – Thermo Electron Corporation), and O_3 was measured using a UV photometric analyzer (Model 49C, TEC). Nitric oxide (NO) and NO_2 were measured using a commercial chemiluminescence analyzer equipped with a molybdenum oxide catalytic converter. Fine particulate matter was also collected using a four-channel $PM_{2.5}$ sampler (RAAS 2.5-400, Thermo Andersen) and was followed by a chemical analysis of the inorganic water-soluble ions (ICS-90, Dionex), OC and EC (Sunset-DOSCOCEC, Sunset Lab), and trace elements (X-ray fluorescence). In addition, the ambient temperature and relative humidity were measured using a portable automatic meteorological station. The visibility data used in this study were obtained from the Weather Underground, with a resolution of 3 h. These data agreed well with those obtained from visual inspection during the sampling periods.

2.3. Data processing

The cut point of the MOUDI is defined as a diameter with aerosol collection efficiency of 50% (Marple et al., 1991), which means that the collected particles in each size bin exhibit an approximately normal distribution against the particle diameter on a logarithmic scale. In this study, the geometric mean value of the two cut-point diameters was used as the average diameter of particles within the size range, and $dC/d\log_{10}Dp$ was calculated to represent the size-resolved concentrations in figures with an *X* axis of particle diameter on a logarithmic scale. To simplify the calculation, the particle modes were divided directly by the cut points. The condensation-mode particles were designated within the size range of 0.18–0.56 μm, droplet-mode particles were within 0.56–1.8 μm and coarse-mode particles were within 1.8–100 μm.

3. Results and discussions

3.1. Size-resolved aerosol composition

The size-segregated aerosol mass concentrations during the sampling periods are depicted in Fig. 2. As shown, the atmospheric

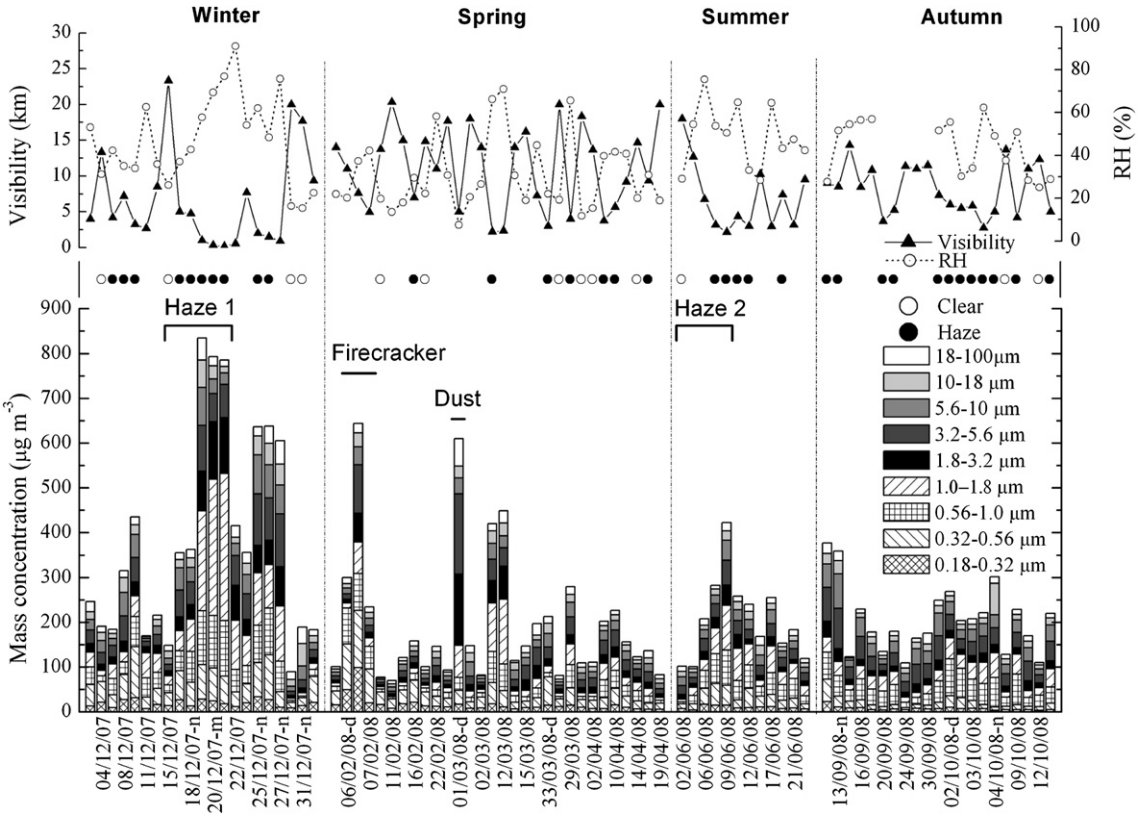

Fig. 2. The time series of size-segregated aerosol mass concentration, visibility and relative humidity together with the division of clear day or haze episode during the sampling periods. The samples are identified as dd/mm/yy-x, where x denotes the sampling time with d as daytime, n as night-time, m as morning and a as afternoon.

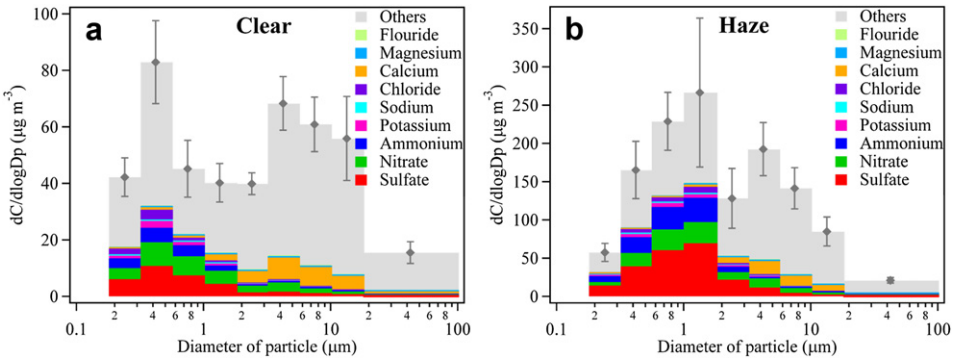

Fig. 3. Size-resolved aerosol compositions for (a) clear days ($n = 13$) and (b) haze episodes ($n = 34$). The marker shows the average mass concentration in each size bin with the error bar representing 1/3 of the standard deviation.

concentrations of PM in Jinan possessed a large variance. Both light and heavy particulate pollution episodes were observed in all four seasons. With a definition of a "clear" day as having all 3-h visibility above 10 km and "haze" as having all 3-h visibility below 10 km without any extreme weather event of fog, rain or snow, 13 sets of size-resolved aerosol samples were collected during clear days and 34 sets were collected during haze episodes (marked in Fig. 2). Most of the remaining sampling days featured haze pollution during part of the day and clear weather in the remaining time. In addition to the haze episodes, heavy PM pollution also occurred during the firecracker episodes (on the Chinese New Year's Eve and on the New Year's Day) and during a dust event (on 1 March 2008).

Fig. 3 compares the averaged aerosol compositions in different size bins for clear days and haze episodes. Generally, particulate matter was found in moderately low concentrations on clear days and was distributed evenly in the fine and coarse modes. The fine particles exhibited a concentration peak in the condensation mode with a mean aerodynamic diameter of 0.42 μm. The secondary inorganic components of sulfates, nitrates and ammonium (SNA) accounted for 32% of the mass concentration of $PM_{1.8}$. Compared with clear days, the average PM concentration almost tripled in haze episodes, with a higher ratio of $PM_{1.8}$ to TSP – 54%. A sharp increase in the aerosol concentration occurred in the droplet mode (0.56–1.8 μm) and the concentration peak for fine mode particles shifted to a larger size – 1.3 μm. Moreover, the fraction of SNA in $PM_{1.8}$ rose to 48%. We have noticed that the droplet-mode particles exhibit a flat concentration peak in relatively clean areas in North America and that the mean aerodynamic diameters are always below 1 μm for the MOUDI data (e.g., Mather et al., 2003; Kleeman et al., 2008; Yao and Zhang, 2011). While in the polluted environment in China, the concentration peaks for droplet-mode particles are sharp, and they always cover a broad size range from 0.56 to 1.8 μm (Hu et al., 2005; Huang et al., 2006; Guo et al., 2010). Compared to North America, the larger size of droplet-mode aerosols in polluted areas of China is believed to be associated with much higher levels of precursory air pollutants including both gases and particles.

Both on clear and hazy days in Jinan, the fine ammonium was found to be well correlated with the fine sulfates and nitrates (Fig. 4). The molar concentrations of ammonium in fine particles were higher than the molar concentrations of sulfates, and the excess ammonium ($NH_4^+ - 2{*}SO_4^{2-}$) almost equaled to the amount of nitrates, indicating the fine ammonium primarily combined with sulfates and nitrates in the forms of $(NH_4)_2SO_4$ and NH_4NO_3, respectively. While in coarse particles, ammonium was scarce, and the sulfates and nitrates always coexisted with crustal species like calcium (see Fig. 3).

3.2. Humidity dependence of droplet aerosol formation

By examining the corresponding RH (also shown in Fig. 2) for each aerosol sample, it is found that the mass concentration of droplet-mode aerosols (within the size range of 0.56–1.8 μm) was prone to increasing in humid weather, e.g., on the heavy hazy days

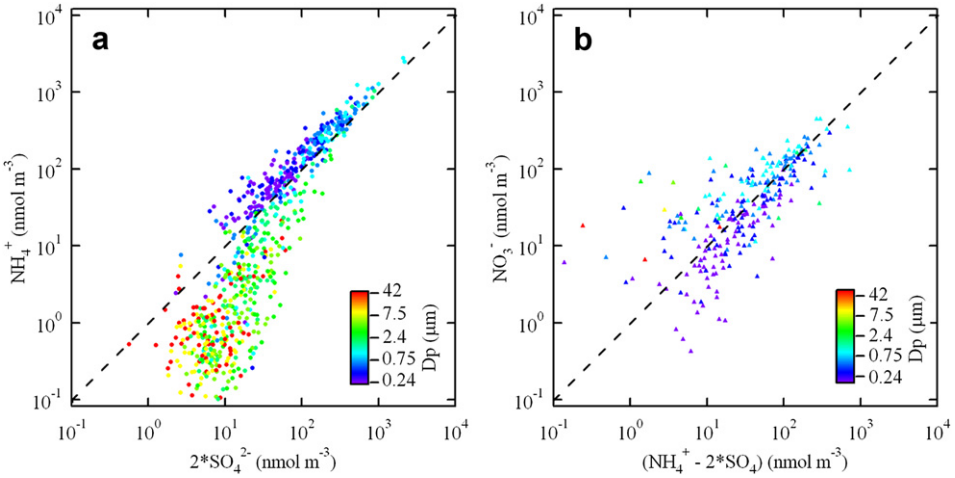

Fig. 4. Scatter plots of molar concentration of (a) NH_4^+ versus $2{*}SO_4^{2-}$ and (b) NO_3^- versus ($NH_4^+ - 2{*}SO_4^{2-}$), color coded by the aerodynamic diameter of particles. Note that all samples are included except those collected in the firecracker episodes and dust event. (For interpretation of the references to colour in this figure legend, the reader is referred to the web version of this article.)

on 19 and 20 December 2007. During all sampling periods, the ambient RH was generally lower than 80% and there was no fog. In the droplet-mode aerosols, abundant highly hygroscopic NH_4NO_3 significantly reduced the deliquescence RH to below 60% (Wexler and Seinfeld, 1991; Tang and Munkelwitz, 1993). Subsequent calculation using an aerosol thermodynamic model of E-AIM II (Extended Aerosol Inorganic Model, http://www.aim.env.uea.ac.uk/aim/aim.php) (Clegg et al., 1998) shows that liquid water can exist in droplet-mode aerosols even at an ambient RH of 20% (Fig. 5a). Generally, the mass ratio of liquid water to the droplet-mode particles was lower than 30% in this study; therefore, the moisture absorption had only a minor influence on the aerosol size. However, the aqueous phase on the aerosol surfaces provided the possibility of the heterogeneous gas–liquid conversion of gaseous precursors such as SO_2, HNO_3, N_2O_5, NO_x and NH_3 to produce secondary inorganic aerosols in the droplet mode at a fast rate.

To investigate the effects of humidity on the droplet-mode aerosol formation, scatter plots were shown of the droplet-mode SNA concentration, the ratio of droplet-mode SNA to total SNA, the fraction of SNA in droplet-mode particles and the MMAD (mass median aerodynamic diameter) of SNA versus the RH in Fig. 5b, c, d and e, respectively. The relationships between them were also given in the figures, which provide potential parameterized formulas for modeling studies of the secondary formation and size distribution of inorganic aerosols in this area. There was light rain for 4 h on the day with highest RH of 91% (22 December 2007); thus, the data point for that day was excluded from Fig. 5b & c. As observed in the figure, the droplet-mode SNA concentration was enhanced with rising RH. If the average RH was below 50%, the droplet-mode SNA concentration was generally lower than 40 μg m^{-3}. Once the RH was above 50%, the concentration of droplet-mode SNA increased sharply, with a maximum of 251 μg m^{-3} at the RH of 77%. Under very dry conditions, e.g., RH < 20%, only a small part (<30%) of SNA were produced in the droplet mode (see Fig. 5c). When the RH was above 50%, more than half of the SNA formed in the droplet mode. The ratio of the droplet-mode SNA to the total SNA (SNA-DL/SNA-total) tended to rise logarithmically with ascending RH. A logarithmic relationship is also found between the fraction of SNA in droplet-mode particles and the RH, and the fraction increased to over 45% when the RH

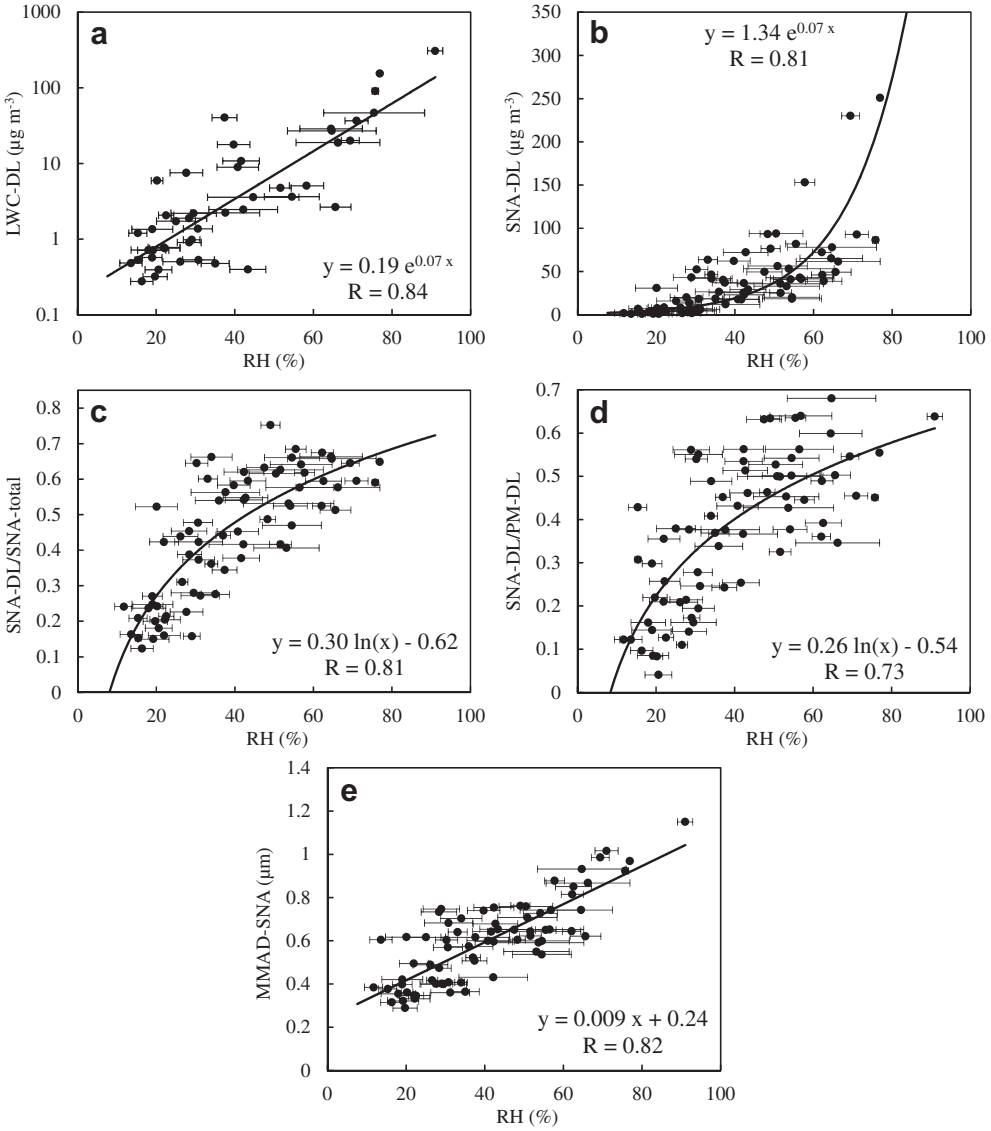

Fig. 5. Scatter plots of (a) liquid water content (LWC) in droplet-mode particles versus RH, (b) droplet-mode SNA concentration versus RH, (c) ratio of droplet-mode SNA to total SNA versus RH, (d) fraction of SNA in droplet-mode particles versus RH and (e) MMAD of SNA versus RH. Note that all data are included here except those collected during the dust event and that the error bar stands for 1/2 standard deviation.

was above 50% (Fig. 5d). Apparently, the elevated SNA-DL/SNA-total ratio in humid conditions would lead to the growth of particle size in the fine mode. As shown in Fig. 5e, the MMAD of SNA grew linearly with the RH. When the RH was 20%, 50% and 80%, the MMAD of SNA was approximately 0.4, 0.7 and 1.0 μm, respectively. In summary, the humidity-related heterogeneous aqueous reactions significantly enhanced the SNA concentrations and their fractions in droplet-mode aerosols under haze conditions and thus played an important role in the secondary formation of droplet-mode aerosols.

The heterogeneous formation of secondary aerosols is associated with the abundances of gas precursors, the aerosol surface area, the aerosol composition and the liquid water content in aerosols. In the urban area of Jinan, intensive source emissions lead to high levels of SO_2, NO_x and ammonia as well as to elevated aerosol loading. The gas precursors are relatively abundant and the aerosol surface area is relatively large, and thus the aerosol water content acts as the limiting factor for the occurrence of the heterogeneous uptake of gas precursors on the aerosol surface. Therefore, the heterogeneous formation of secondary aerosols enhances as the RH increases. During haze episodes in Jinan, the humidity was moderate or high; therefore, a large amount of secondary sulfates and nitrates were produced in the droplet mode and their fractions in aerosols increased.

3.3. Secondary aerosol formation during haze episodes

Haze pollution, featuring an enhanced fine aerosol loading and an elevated fraction of ammoniated sulfates and nitrates, was frequently observed in Jinan in all four seasons (Cheng et al., 2011b). During the sampling periods of this study, two multi-day, severe-haze episodes occurred in winter (17–20 December 2007) and summer (8–10 June 2008). The size-resolved aerosol samples were densely collected during these two haze episodes, which provided an opportunity to investigate the formation mechanism of secondary sulfates and nitrates along with the causal factors. For each time period when size-segregated aerosol samples were collected, the corresponding atmospheric visibility, weather conditions and air pollutant concentrations/parameters are listed in Table 1. Particularly, the visibility was reduced to 0.6 km in the afternoon of 20 December 2007, with an extremely high $PM_{1.8}$ of 532 μg m^{-3}. Because the data of ambient concentrations of SO_2 and NO_x were not available in the winter campaign, they were not included in Table 1. During the summer haze episode from 2 to 9 June (also including the clear days before the haze episode), SO_2 and NO_x showed moderate and irregular variance. It is noted that the air mass was relatively stable, characterized by generally low wind speeds during both haze episodes.

3.3.1. Secondary formation of sulfates

Fig. 6a & b clearly demonstrate the continuous increase of sulfate concentrations during the multi-day haze episodes. At the early stage, sulfates exhibited a flat concentration peak in the condensation mode with a size range of 0.32–0.56 μm (i.e., on 17 December 2007 and 2 June 2008). Following with aggravated particle pollution, droplet-mode sulfates increased remarkably, whereas condensation-mode sulfates showed only a slight increase. In the last stage of the haze episodes, the sulfate concentration peak became sharper and shifted to a larger size – droplet mode – compared with clear days in the beginning. During the haze episodes, sulfates exhibited an obvious positive increase in the droplet mode (0.56–1.8 μm) (see Fig. 6c & d). The integrated rate of increase of sulfates in $PM_{1.8}$ varied from 0.3 to 4.1 μg m^{-3} h^{-1} in the winter haze episode and from 0.2 to 1.0 μg m^{-3} h^{-1} in the summer haze episode. Furthermore, the fraction of sulfates in droplet-mode particles consistently became higher – from approximately 10% and gradually increasing to 30%. The particle size of sulfates became progressively larger, with the MMAD increasing from approximately 0.4 to 1.0 μm (Fig. 6e & f). The elevated sulfate concentration and the elevated fraction of sulfates in droplet-mode particles point to the intensive secondary formation of droplet-mode sulfates under haze conditions.

The examination of weather conditions shows that the relative humidity gradually increased during the multi-day haze episodes (listed in Table 1). A remarkable secondary formation of droplet mode sulfates primarily resulted from the heterogeneous aqueous reactions of SO_2 on existing aerosols followed by subsequent oxidation. During the winter in Jinan, the ambient O_3 concentrations were quite low (see Table 1) due to the low light intensity and a weak photochemical effect. The H_2O_2 concentration should also be at a very low level because of the weak solar radiation in the cold season and the abundant NO_x in urban areas (Kang et al., 2002). Under such conditions, SO_2 oxidation in the aqueous layer on aerosol surface was unlikely to be dominated by photochemical oxidants. In addition, the rate of increase of sulfate concentration rose with an increasing content of iron and magnesium in fine particles (Table 1). Therefore, the sharp increase of droplet-mode sulfates during the haze episode in winter is considered to be dominated by the aqueous catalytic oxidation by oxygen together with iron and manganese (Martin and Good, 1991). The iron concentration increased significantly, while the calcium concentration showed little change, which indicates that the abundant iron in fine particles were primarily emitted from steel smelting and coal combustion instead of ground dusts. Moreover, the increased iron content on 9 June 2008 corresponded to the highest rate of increase of sulfates during the summer haze episode, which suggests that the catalytic oxidation involving in iron and manganese contributed to the fast formation of droplet-mode sulfates in

Table 1
The visibility, weather conditions and air pollutant concentrations/parameters for selected multi-day haze episodes in winter and summer.

Season	Sample ID[a]	Visi. (km)	T (°C)	RH (%)	O_3 (ppb)	Ca[b] (μg m^{-3})	Fe[b] (μg m^{-3})	Mn[b] (μg m^{-3})	OC/EC[b]
Winter	15/12/07	25.4	3.5	26.1	7.8	0.7	1.3	0.10	5.0
	17/12/07	14.4	6.3	37.0	6.9	1.7	1.6	0.13	5.8
	18/12/07-n	11.8	5.6	42.7	8.3	0.8	1.3	0.14	7.8
	19/12/07-d	2.4	5.1	57.7	6.4	1.4	2.6	0.20	7.6
	20/12/07-m	2.4	1.5	69.4	4.6	1.0	5.5	0.36	8.3
	20/12/07-a	0.6	0.1	76.9	5.4	0.9	3.2	0.34	8.4
Summer	02/06/08	23.4	22.3	29.0	38.3	1.1	0.8	0.04	
	04/06/08	15.0	20.3	54.5	48.1	0.6	0.7	0.03	4.0
	06/06/08	7.3	20.6	75.4	15.4	1.0	1.4	0.10	5.1
	08/06/08	7.1	26.3	53.7	58.2				6.4
	09/06/08	7.2	27.2	50.5	38.2	1.5	2.4	0.13	6.7

[a] The "n" stands for night-time, "d" for daytime, "m" for morning and "a" for afternoon.
[b] The calcium, iron, magnesium concentrations and the OC/EC ratio were for $PM_{2.5}$.

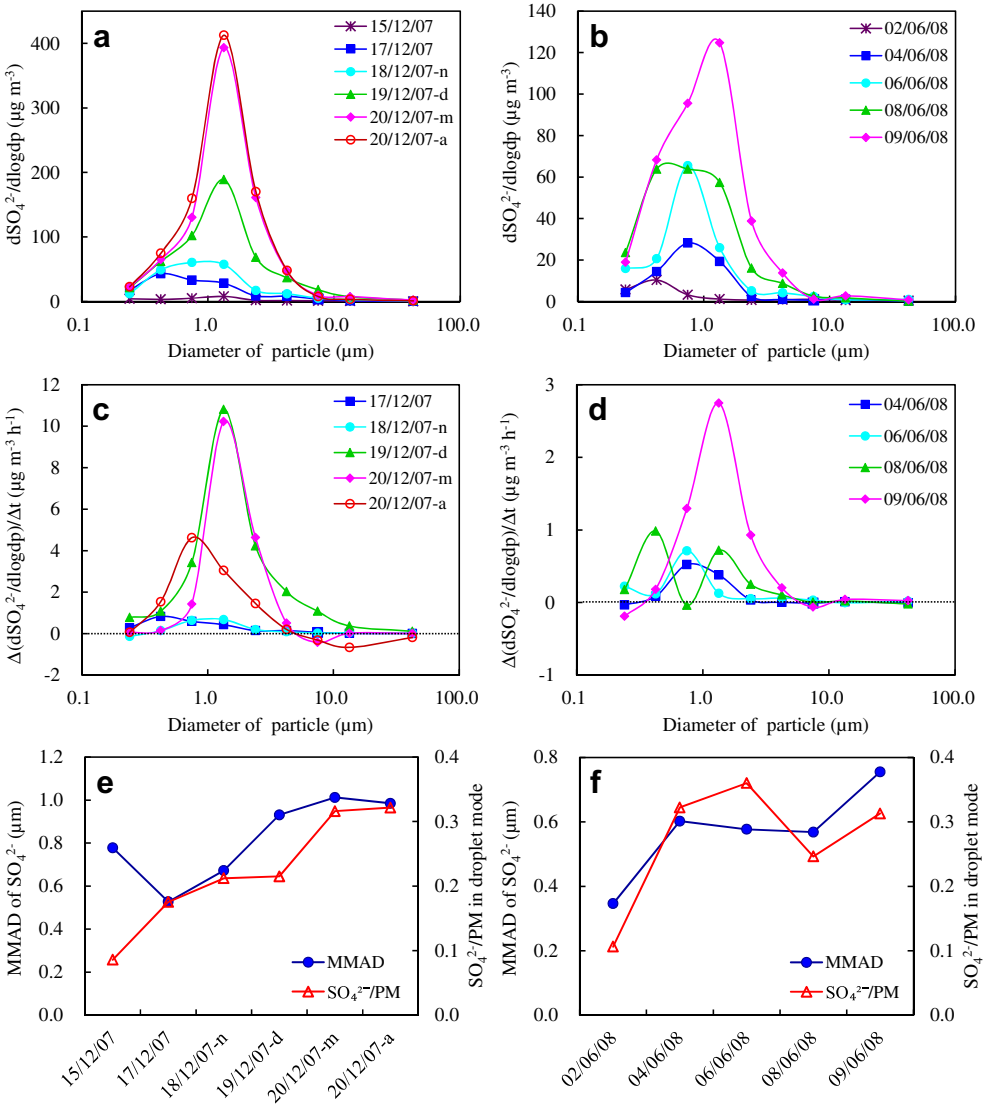

Fig. 6. Size distributions of the sulfate concentration and their rate of increase, variations of the sulfate MMAD and the sulfate fraction in droplet-mode particles for the selected multi-day haze episodes in (a, c & e) winter and (b, d & f) summer. Note: *increase rate* = $(C_n - C_{n-1})/(t_n - t_{n-1})$, with n standing for sample ID, C for concentration and t for the starting time of the sampling.

the hot season. The sulfates primarily formed in the droplet mode, and thus the concentration peak (and the MMAD) shifted to the droplet mode. During summer in Jinan, photochemical oxidant concentrations were relatively high because of the intense solar radiation together with the abundant precursors. In this condition, the homogeneous reaction of SO_2 with the OH radical followed by condensational growth also contributed to secondary sulfate formation; e.g., the daily average O_3 was 58.2 ppb on 8 June 2008 and an apparent increase was observed for the condensation-mode sulfates.

Additionally, the OC/EC ratio in the fine particles increased on heavily polluted hazy days (also shown in Table 1), which indicates relatively aged air masses from the regional-scale (Pio et al., 2011). The long-lived air mass during the haze episode was also favorable for the aerosols to grow to a larger size through coagulation and coalescence.

3.3.2. *Secondary formation of nitrates*

As shown in Fig. 7a & b, a remarkable increase of nitrates was also observed during the multi-day haze episodes. On clear days in the beginning, the fine nitrates exhibited a concentration peak in the condensation mode, whereas the coarse nitrates exhibited a moderately small peak in size range of 3.2–5.6 μm. With the aggravation of the haze episode, droplet-mode nitrates apparently increased and the concentration peak of fine nitrates shifted to a larger size – the droplet mode. The coarse nitrates were also enhanced by a small degree, possibly due to more abundant precursors and the accumulation of pollutants on hazy days. Compared to the sulfates, the temporal variation of fine nitrates was less consistent with the rising RH, which indicates that some other factors were likely to influence the formation processes of secondary nitrates. The rate of increase of $PM_{1.8}$ nitrates was generally low, with a maximum of 1.5 μg m^{-3} h^{-1} observed on 19 December 2007 (Fig. 7c & d). During the haze episode, the MMAD of nitrates rose gradually, from 0.44 to 0.96 μm in winter and from 0.62 to 0.93 μm in summer (see Fig. 7e & f). However, the fraction of nitrates in the droplet-mode particles did not undergo a continuous increase and always dropped back to below 10% on the heavily polluted hazy days. These suggest that the secondary formation of fine nitrates was suppressed under certain conditions.

As mentioned earlier, fine nitrates in Jinan always combined with ammonium in the form of NH_4NO_3; therefore, under haze

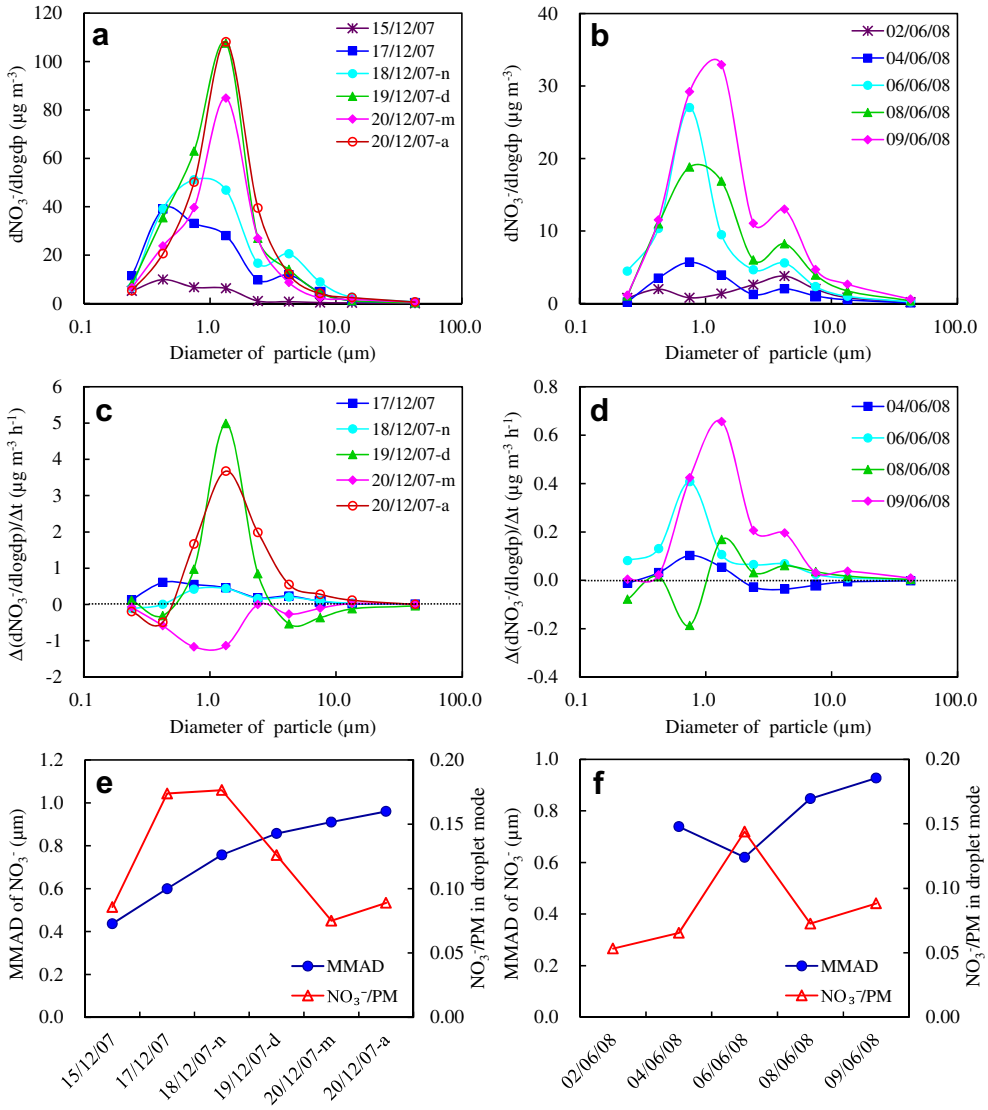

Fig. 7. Size distributions of the nitrate concentration and their rate of increase, variations of the nitrate MMAD and the nitrate fraction in droplet-mode particles for the selected multi-day haze episodes in (a, c & e) winter and (b, d & f) summer.

conditions, the droplet-mode nitrates are believed to form primarily via the heterogeneous aqueous reaction of gaseous nitric acid (HNO_3) and ammonia (NH_3) on the wet surfaces of pre-existing aerosols. As we know, the NH_4NO_3 in fine particles readily establishes a temperature- and humidity-dependent equilibrium with gaseous HNO_3 and NH_3 (Stelson and Seinfeld, 2007). During the summer haze episode, the ambient temperature was high and varied from 20.3 to 27.2 °C (shown in Table 1). Under this condition, the aerosol NH_4NO_3 readily dissociated into HNO_3 and NH_3, and the dissociation amplified with rising temperature and descending RH (Seinfeld and Pandis, 2006). The highest fraction of nitrates in droplet-mode particles (14%) occurred on 6 June 2008, with nearly the lowest temperature and highest RH occurring during that day. This result indicates that low temperature and high humidity were favorable to the secondary formation of fine nitrates in the droplet mode, whereas the secondary formation would be suppressed at high ambient temperatures during summer. In contrast, the temperature during the winter haze episode was rather low, ranging from 0.1 to 6.3 °C. In such conditions, the particulate NH_4NO_3 hardly decomposed, and the HNO_3 tended to react with NH_3 to produce NH_4NO_3. During winter in Jinan, the weak solar radiation would reduce the photochemical production of HNO_3. Furthermore, the ammonia emission was generally low in the cold season and was prone to decrease at lower temperature (Shen et al., 2011). Therefore, the temperature was possibly the dominating factor that limited the fine nitrate formation in winter. For the aerosol samples on the days of 17–19 December 2007, the elevated concentration of droplet nitrates and their rising contribution to particulate matter demonstrate the increased secondary formation of droplet-mode nitrates at high temperature in the winter haze episode. The low temperature suppressed the further production of fine nitrate (e.g., the samples on 20 December 2007) due to a lack of nitric acid and ammonia.

4. Summary and conclusion

Size-segregated aerosols were collected using a MOUDI at the urban area of Jinan, China, from December 2007 to October 2008, and the water-soluble components were subsequently analyzed by ion chromatography. The size-resolved aerosol ionic composition in haze episodes was characterized by sharply increased SNA in the droplet mode (0.56–1.8 μm), which was substantially different

from that on clear days. Under haze conditions, most of the fine sulfates and nitrates coexisted with the ammonium in the forms of $(NH_4)_2SO_4$ and NH_4NO_3, respectively. Abundant NH_4NO_3 in fine particles reduced the deliquescence relative humidity, which provided the possibility of secondary inorganic aerosol formation through the heterogeneous aqueous uptake of precursory gases at moderate humidity. The secondary formation of droplet-mode SNA through heterogeneous aqueous reactions strongly relied on the relative humidity. Once the ambient humidity rose, the concentration of droplet-mode SNA apparently increased. The ratio of the droplet-mode SNA to total SNA and the fraction of SNA in droplet-mode particles also increased logarithmically with increasing RH. When the RH was above 50%, more than half of the SNA was produced in the droplet mode, and the SNA comprised over 45% of the droplet-mode aerosols. Case studies of haze episodes indicate that the secondary sulfates in the droplet mode were associated with the heterogeneous oxidation of SO_2 under catalysis by iron and manganese, which was emitted from the local steel smelting and coal combustion. The secondary formation of droplet-mode nitrates was correlated with the temperature-dependent thermodynamic equilibrium of NH_4NO_3 with gaseous nitric acid and ammonia. Under moderately high temperatures during summer, increased temperature led to greater decomposition of ammonium nitrates and thus suppressed the fine nitrate formation. By contrast, the ambient temperature in winter was generally low in Jinan. The rising temperature resulted in enhanced nitric acid formation and ammonia emission, and thus elevated the fine nitrate content.

Acknowledgments

The authors thank Jin Wang for his help in organizing the field study. We also thank Chao Yuan, Zheng Xu, Youping Shou and Jing Wang for their help in the laboratory work. This research was funded by the Shandong Provincial Environmental Protection Department (Project 2006045) and the National Basic Research Program of China (973 Project No. 2005CB422203).

References

Berresheim, H., Jaeschke, W., 1986. Study of metal aerosol systems as a sink for atmospheric SO_2. Journal of Atmospheric Chemistry 4, 311–334.

Buzcu, B., Yue, Z.W., Fraser, M.P., Nopmongcol, U., Allen, D.T., 2006. Secondary particle formation and evidence of heterogeneous chemistry during a wood smoke episode in Texas. Journal of Geophysical Research 111, D10S13. http://dx.doi.org/10.1029/2005jd006143.

Cheng, S., Yang, L., Zhou, X., Wang, Z., Zhou, Y., Gao, X., Nie, W., Wang, X., Xu, P., Wang, W., 2011a. Evaluating $PM_{2.5}$ ionic components and source apportionment in Jinan, China from 2004 to 2008 using trajectory statistical methods. Journal of Environmental Monitoring 13, 1662–1671.

Cheng, S., Yang, L., Zhou, X., Xue, L., Gao, X., Zhou, Y., Wang, W., 2011b. Size-fractionated water-soluble ions, situ pH and water content in aerosol on hazy days and the influences on visibility impairment in Jinan, China. Atmospheric Environment 45, 4631–4640.

Clegg, S.L., Brimblecombe, P., Wexler, A.S., 1998. Thermodynamic model of the system $H^+-NH_4^+-SO_4^{2-}-NO_3^--H_2O$ at tropospheric temperatures. The Journal of Physical Chemistry A 102, 2137–2154.

Feng, Y., Penner, J.E., 2007. Global modeling of nitrate and ammonium: interaction of aerosols and tropospheric chemistry. Journal of Geophysical Research 112, D01304. http://dx.doi.org/10.1029/2005jd006404.

Guo, S., Hu, M., Wang, Z.B., Slanina, J., Zhao, Y.L., 2010. Size-resolved aerosol water-soluble ionic compositions in the summer of Beijing: implication of regional secondary formation. Atmospheric Chemistry and Physics 10, 947–959.

Haywood, J., Bush, M., Abel, S., Claxton, B., Coe, H., Crosier, J., Harrison, M., Macpherson, B., Naylor, M., Osborne, S., 2008. Prediction of visibility and aerosol within the operational Met Office Unified Model. II: validation of model performance using observational data. Quarterly Journal of the Royal Meteorological Society 134, 1817–1832.

Hu, M., Zhao, Y., He, L., Huang, X., Tang, X., Yao, X., Chan, C., 2005. Mass size distribution of Beijing particulate matters and its inorganic water-soluble ions in winter and summer. Environmental Science 26, 1–6 (in Chinese with abstract in English).

Huang, X.F., Yu, J., He, L.Y., Yuan, Z., 2006. Water-soluble organic carbon and oxalate in aerosols at a coastal urban site in China: size distribution characteristics, sources and formation mechanisms. Journal of Geophysical Research 111, D22212. http://dx.doi.org/10.1029/2006JD007408.

John, W., Wall, S.M., Ondo, J.L., Winklmayr, W., 1990. Modes in the size distributions of atmospheric inorganic aerosol. Atmospheric Environment 24, 2349–2359.

Kang, C.M., Han, J.S., Sunwoo, Y., 2002. Hydrogen peroxide concentrations in the ambient air of Seoul, Korea. Atmospheric Environment 36, 5509–5516.

Kleeman, M.J., Riddle, S.G., Jakober, C.A., 2008. Size distribution of particle-phase molecular markers during a severe winter pollution episode. Environmental Science & Technology 42, 6469–6475.

Li, W., Zhou, S., Wang, X., Xu, Z., Yuan, C., Yu, Y., Zhang, Q., Wang, W., 2011. Integrated evaluation of aerosols from regional brown hazes over northern China in winter: concentrations, sources, transformation, and mixing states. Journal of Geophysical Research 116, D09301. http://dx.doi.org/10.1029/2010jd015099.

Liu, S., Hu, M., Slanina, S., He, L.Y., Niu, Y.W., Bruegemann, E., Gnauk, T., Herrmann, H., 2008. Size distribution and source analysis of ionic compositions of aerosols in polluted periods at Xinken in Pearl River Delta (PRD) of China. Atmospheric Environment 42, 6284–6295.

Marple, V.A., Rubow, K.L., Behm, S.M., 1991. A Microorifice Uniform Deposit Impactor (MOUDI): description, calibration and use. Aerosol Science and Technology 14, 434–446.

Martin, L.R., Good, T.W., 1991. Catalyzed oxidation of sulfur dioxide in solution: the iron–manganese synergism. Atmospheric Environment 25, 2395–2399.

Mather, T., Allen, A., Oppenheimer, C., Pyle, D., McGonigle, A., 2003. Size-resolved characterisation of soluble ions in the particles in the tropospheric plume of Masaya volcano, Nicaragua: origins and plume processing. Journal of Atmospheric Chemistry 46, 207–237.

Nie, W., Wang, T., Gao, X.M., Pathak, R.K., Wang, X.F., Gao, R., Zhang, Q.Z., Wang, W.X., 2010. Comparison of three filter-based and a continuous technique for measuring atmospheric fine sulfate and nitrate. Atmospheric Environment 44, 4396–4403.

Pathak, R.K., Wu, W.S., Wang, T., 2009. Summertime $PM_{2.5}$ ionic species in four major cities of China: nitrate formation in an ammonia-deficient atmosphere. Atmospheric Chemistry and Physics 9, 1711–1722.

Pio, C., Cerqueira, M., Harrison, R.M., Nunes, T., Mirante, F., Alves, C., Oliveira, C., Sanchez de la Campa, A., Artíñano, B., Matos, M., 2011. OC/EC ratio observations in Europe: re-thinking the approach for apportionment between primary and secondary organic carbon. Atmospheric Environment 45, 6121–6132.

Salma, I., Balashazy, I., Winkler-Heil, R., Hofmann, W., Zaray, G., 2002. Effect of particle mass size distribution on the deposition of aerosols in the human respiratory system. Journal of Aerosol Science 33, 119–132.

Schryer, D.R., 1982. Heterogeneous Atmospheric Chemistry. American Geophysical Union.

Seinfeld, J.H., Pandis, S.N., 2006. Atmospheric Chemistry and Physics: From Air Pollution to Climate Change, second ed. John Willey & Sons, Inc., New York.

Shen, J., Liu, X., Zhang, Y., Fangmeier, A., Goulding, K., Zhang, F., 2011. Atmospheric ammonia and particulate ammonium from agricultural sources in the North China Plain. Atmospheric Environment 45, 5033–5041.

Stelson, A.W., Seinfeld, J.H., 2007. Relative humidity and temperature dependence of the ammonium nitrate dissociation constant. Atmospheric Environment 41 (Suppl.), 126–135.

Sun, Y., Zhuang, G., Tang, A., Wang, Y., An, Z., 2006. Chemical characteristics of $PM_{2.5}$ and PM_{10} in haze–fog episodes in Beijing. Environmental Science & Technology 40, 3148–3155.

Tan, J., Duan, J., Chen, D., Wang, X., Guo, S., Bi, X., Sheng, G., He, K., Fu, J., 2009. Chemical characteristics of haze during summer and winter in Guangzhou. Atmospheric Research 94, 238–245.

Tang, I.N., Munkelwitz, H.R., 1993. Composition and temperature dependence of the deliquescence properties of hygroscopic aerosols. Atmospheric Environment 27, 467–473.

Turšič, J., Berner, A., Veber, M., Bizjak, M., Podkrajšek, B., Grgić, I., 2003. Sulfate formation on synthetic deposits under haze conditions. Atmospheric Environment 37, 3509–3516.

Wang, Y., Zhuang, G., Sun, Y., An, Z., 2006. The variation of characteristics and formation mechanisms of aerosols in dust, haze, and clear days in Beijing. Atmospheric Environment 40, 6579–6591.

Wang, X., Zhang, Y., Chen, H., Yang, X., Chen, J., Geng, F., 2009. Particulate nitrate formation in a highly polluted urban area: a case study by single-particle mass spectrometry in Shanghai. Environmental Science & Technology 43, 3061–3066.

Wexler, A.S., Seinfeld, J.H., 1991. Second-generation inorganic aerosol model. Atmospheric Environment 25, 2731–2748.

Wu, D., 2006. More discussions on the differences between haze and fog in city. Meteorological Monthly 32, 9–15 (in Chinese with abstract in English).

Yang, L., Wang, D., Cheng, S., Wang, Z., Zhou, Y., Zhou, X., Wang, W., 2007. Influence of meteorological conditions and particulate matter on visual range impairment in Jinan, China. Science of the Total Environment 383, 164–173.

Yao, X.H., Zhang, L., 2011. Sulfate formation in atmospheric ultrafine particles at Canadian inland and coastal rural environments. Journal of Geophysical Research 116, D10202. http://dx.doi.org/10.1029/2010jd015315.

Ye, X., Ma, Z., Zhang, J., Du, H., Chen, J., Chen, H., Yang, X., Gao, W., Geng, F., 2011. Important role of ammonia on haze formation in Shanghai. Environmental Research Letters 6, 024019.